PHYSICAL REVIEW E **79**, 040401(R) (2009)

Effect of network topology on phase separation in two-dimensional Lennard-Jones networks

Orit Peleg,[1,*,†] Martin Kröger,[1,‡] and Yitzhak Rabin[2,§]
[1]*Department of Materials, Polymer Physics, ETH Zürich, Wolfgang-Pauli-Strasse 10, CH-8093 Zürich, Switzerland*
[2]*Department of Physics, Nano-materials Research Center, Institute of Nanotechnology and Advanced Materials, Bar-Ilan University, Ramat-Gan 52900, Israel*

(Received 24 December 2008; published 6 April 2009)

We generate two-dimensional Lennard-Jones networks with random topology by preparing a perfect four-functional network of identical harmonic springs and randomly cutting some of the springs. Using molecular-dynamics simulations we find that the fraction p of active springs affects both the temperature of phase separation and the type of structures observed below this temperature, from networklike high-density patterns at $p>0.5$ ("gel") to dropletlike structures at $p<0.5$ ("sol"). In the gel domain, these patterns are determined by the interplay between free energy and network topology, with the former dominant as $p\to 1$ and the latter as $p\to 0.5$.

DOI: 10.1103/PhysRevE.79.040401 PACS number(s): 82.70.Gg, 64.70.K−, 82.20.Wt

Recently we introduced and studied (by molecular-dynamics simulations) a simple elastic Lennard-Jones (LJ) model of phase separation in gels in which the gel is treated as a stretched network of particles connected by harmonic springs and interacting through LJ forces [1,2]. We considered only perfectly connected (four and six functional) networks in two-dimensional (2D) and analyzed their behavior as a function of temperature, T, and spring coefficient, k. In the above work as well as in previous studies of microphase separation in polymer gels [3,4], no attempt was made to introduce one of the salient characteristics of real polymer networks: because the process of cross-linking is random, the distribution of cross-links which determines the topology of the networks is highly inhomogeneous, and this structural inhomogeneity is frozen once and for all during the process of gelation [5–8]. Such effects were studied by Brownian dynamics simulations of randomly cross-linked polymer gels in ideal solvent (no phase separation) [9] and of microphase separation in cross-linked polymer blends in poor solvent [10]. In the present work we address phase separation in *randomly cross-linked* 2D networks. The network topology is fixed by discarding (at random) some of the springs in a perfect network. We compute the phase diagram in the (p,T) plane (p is the fraction of the remaining active springs which determines the topology of the network) and study the dependence of the density patterns on the network topology.

In the 2D system all particles interact through a LJ potential $U_{\mathrm{LJ}}(r_{ij})=4\epsilon[(\sigma/r_{ij})^{12}-(\sigma/r_{ij})^{6}]$ where $r_{ij}\equiv|\mathbf{r}_i-\mathbf{r}_j|$ is the time-dependent relative distance between particles i and j, using the cutoff distance $r_{\mathrm{cut}}=3\times 2^{1/6}$. In addition, particles initially being nearest neighbors on the ideal grid permanently interact through a harmonic spring potential $U_{\mathrm{spring}}(r_{ij})=\frac{1}{2}kr_{ij}^2$ where k is the spring coefficient. In order to add randomness to the network, the systems are prepared with a given fraction p of active springs by starting from a perfect four-functional network and randomly deactivating springs until only a fraction p of the initial springs remains [see illustration of the initial state with $p=0.7$ in Fig. 1(a)]. While different realizations (different choices of the eliminated springs) at same p lead to microscopically different configurations, they turn out to be statistically equivalent (see our supporting information [13] for details). We would like to stress that our method of construction of random networks is not unique and that in real gels, the probability of introducing a new cross-link may depend on the local concentration of the existing ones. We apply periodic boundary conditions, which stabilize the connected network by stretching it on a torus [see Fig. 1(a)], thereby creating an effective force which mimics the osmotic pressure in real gels and opposes the contractile action of the spring forces and the LJ forces. Beyond the percolation threshold, $p\gtrapprox 0.5$, the boundary conditions prevent the collapse of the macroscopically connected network and ensure that LJ attractions can only give rise to localized density heterogeneities (microphase separation) at sufficiently low temperatures. The network is thermostatted by controlling the amplitude of the velocities of the particles and studied using molecular-dynamics simulation at various temperatures T and fractions of active springs p in the ranges $T\in[0.2,5]$ and $p\in[0,1]$, respectively, with spring coefficient $k=0.1$, initial grid spacing $g=3.5$, and $N=100\times 100$ particles, with integration time step $\delta t=0.004$. This choice of parameters had been motivated and discussed in [1] where the case $p=1$ had been studied. The purely elastic reference system, our model system in the absence of LJ interactions, had also been studied earlier (see [9]). If the distance between two particles is less than $r_c=1.5$, they are considered to belong to the same cluster (as in [1,2,12]). Using this definition, particles and springs are assigned to phases: a particle is either a member of a cluster and defined to belong to the high-density phase (HDP) or isolated and belongs to the low-density phase (LDP). Springs are "solid" if both particles they connect belong to the HDP, they are "interfacial" if exactly one of the particles is member of the HDP, and "gaseous" otherwise.

We have previously shown [2] that for fully cross-linked LJ network ($p=1$), there exists a critical temperature T^* such that: (1) the decrease in temperature from above to below

*Corresponding author; op@mat.ethz.ch
†Present address: Biozentrum, Swiss Nanoscience Institute, University of Basel, 4056 Basel, Switzerland
‡URL: www.complexfluids.ethz.ch

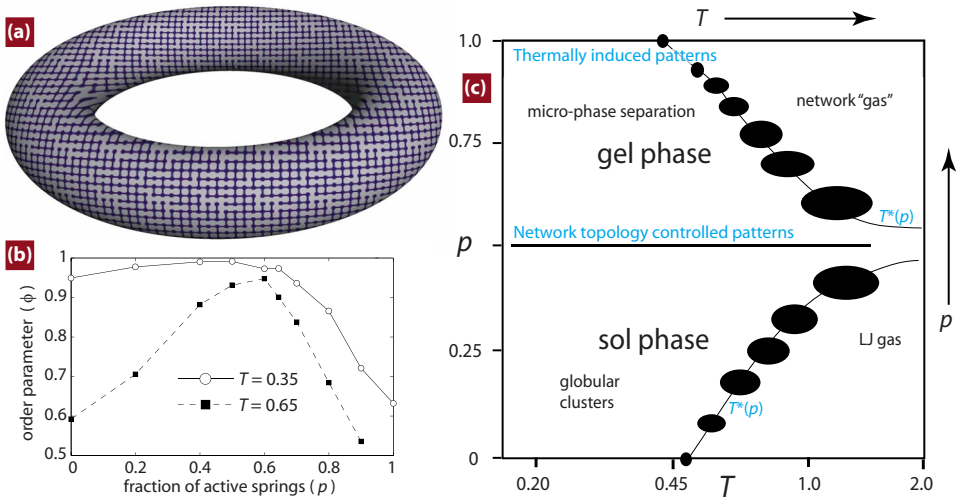

FIG. 1. (Color online) (a) Illustration of a randomly cross-linked initial configuration with a fraction $p=0.7$ of active springs (represented as edges). Elastic springs permanently act between those Lennard-Jones particles (initially located at the nodes) being nearest neighbors on the ideal lattice. For this topology, the bond-percolation threshold is $p\approx 0.5$. (b) Order parameter vs fraction of active springs p for two temperatures $T=0.35$ and $T=0.65$. (c) Phase diagram in the T-p plane (logarithmic scale on the T axis). The gel and the sol phases are divided by the thick solid line, and the ordering transition occurs at T_p^* as function of the fraction p of active springs (ellipsoids represent the size of error bars). The outermost regimes, $p=0$, and $p=1$, had been studied earlier, cf. [11] and [1,2,12], respectively.

$T_{p=1}^*=0.432\pm 0.01$ is accompanied by a dramatic increase in the order parameter ϕ defined as the fraction of particles in the HDP, and (2) for $T>T_{p=1}^*$ only small clusters embedded in a LDP are observed and at temperatures below $T_{p=1}^*$ filamentous structures develop in the system. We find that in the case of randomly cross-linked networks ($p<1$), one can also define a critical temperature T_p^* which depends on the fraction of active springs. However, as will be shown in the following, in this case T_p^* can be defined only via the jump of the order parameter (criterion 1); with decreasing p (in the range $p>0.5$), the shapes of the filamentous structures are increasingly determined by the topology of the network and can be clearly observed even at $T>T_p^*$. Moreover, examining different values of p reveals a different phase separation behavior which will be described next by selected quantities which were collected during the run: the order parameter ϕ [Fig. 1(b)], the fraction of particles in the biggest cluster, the potential energy per particle, and the average distance between neighboring particles in the HDP. All quantities are plotted in Fig. 2(A) as a function of p for two different temperatures, $T=0.35$ ($<T_{p=1}^*$) and $T=0.65$ ($>T_{p=1}^*$). A complete set of configuration snapshots taken in the steady state as well as plots for additional scalar measures are collected in [13].

The phase diagram is shown in Fig. 1(c). The dark solid line $p\approx 0.5$ (the percolation threshold) divides the phase diagram into two main regions: "sol" ($p<0.5$) and "gel" ($p>0.5$). In the limiting cases $p=1$ and $p=0$ we recover known critical temperatures $T_{p=1}^*=0.432\pm 0.01$ [1] and $T_{p=0}^*=0.47\pm 0.01\approx 0.5$ [11] associated with the onsets of pronounced ordering in the fully cross-linked and the uncross-linked systems, respectively. Notice that T^* does not vary monotonously with p [light solid lines in Fig. 1(c)]. This agrees with the expectation that in the gel phase $p>0.5$, T^* decreases with increasing p since the addition of springs increases the number of interfacial springs that connect the clusters to the rest of the network and thus suppresses the formation of HDP clusters. In the sol phase $p<0.5$, the network breaks into small clusters with only internal but no intercluster connections. These internal connections act as effective attractions that promote the formation of high-density clusters, and therefore T^* increases with increasing p.

We now examine the physics of the different regimes in the phase diagram in more detail. Below the percolation threshold ($p<0.5$), the network is not fully connected and increasing p increases the size of connected clusters. At low temperatures this has only a small effect on the distance between particles in the solid phase [Fig. 2(A)], on the number of LJ interactions, and on the number of particles in clusters [Fig. 1(b)] since the effective interaction between particles is dominated by LJ forces. At higher temperatures (but still below T_p^*), elastic forces inside connected clusters dominate over the LJ forces. Since such forces act as effective attraction between particles, increasing p increases the number of particles in dense clusters, reduces the distances between them, and decreases the potential energy. When T exceeds T_p^*, the system behaves as a LJ gas.

Above $p\approx 0.5$ a stretched network is formed. Increasing p increases the elastic forces that oppose the formation of dense localized domains which is accompanied by the stretching of the surrounding network. Therefore, increasing p decreases the number of particles in clusters and increases the interparticle separation in the HDP, thus increasing the potential energy [see Fig. 2(A)] and leading to the observed decrease in T_p^* with increasing p. This physical mechanism was invoked in Ref. [14] to explain the enhancement of light scattering from NIPA/AAc gels in poor solvent, observed at low cross-linking densities. At $p=1$ we have a perfectly connected network with spatially homogeneous topology. When the system is quenched into the microphase separation region at temperatures below $T_{p=1}^*$, the appearance of the resulting

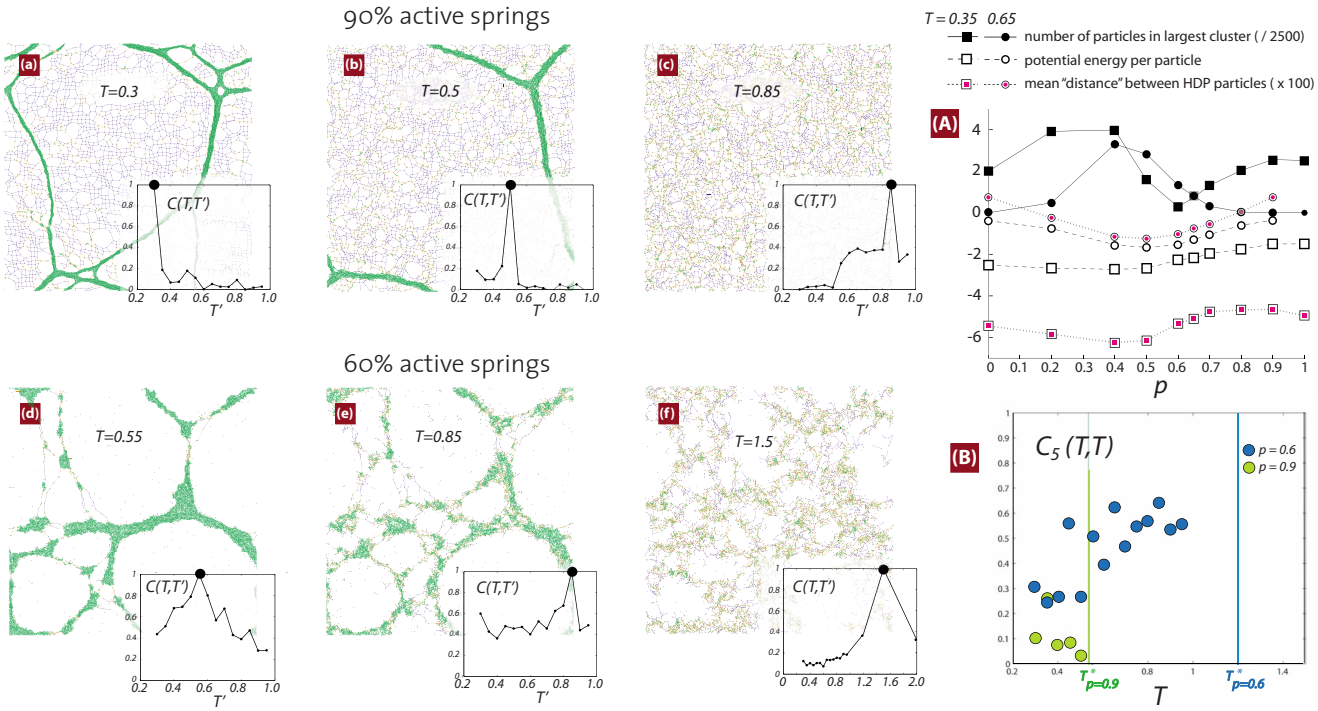

FIG. 2. (Color online) (a)–(f) Correlation between steady states of a network (fixed network topology) at different temperatures. Shown are representative results for (top) $p=0.9$ and (bottom) $p=0.6$. HDP, LDP, and interfacial springs are shown in (dark) green, blue, and (light) yellow, respectively. The density correlation coefficient $C(T,T')$ (see insets) quantifies the relative similarity of configurations in the temperature neighborhood for each shown configuration and carries information about the many pictures omitted from this plot (see [13] for a complete gallery of snapshots). (A) Sample evaluated quantities vs p at two different temperatures (the plotted "*distance*" is true distance minus 1.22). (B) We heated final configurations at given temperature T up to $T'=5$, equilibrated them for a few millions steps, cooled them to the original temperature, and waited for another few million steps. Then we calculated the correlation $C_{T'}(T,T)$ between the final and the original configurations.

filamentous structures is determined by the random locations of spontaneously forming nucleation sites (small high-density clusters) which then coalesce into filaments [1]. With decreasing temperature, the number of nucleation sites increases and the mesh size of the network decreases. Because of the random character of *homogeneous nucleation*, different quenches (from the same initial state to the same final temperature) yield different filamentous structures; yet, the statistical properties of these structures (characteristic correlation length, order parameter, etc.) are identical [2]. When $p<1$, the topology of the network is no longer homogeneous and it is composed of highly cross-linked domains surrounded by weakly connected regions. Since the network is globally stretched, highly cross-linked regions in which restoring elastic forces oppose stretching are denser than the loosely cross-linked ones. As temperature is lowered, there is competition between free-energy-driven reorganization of the network and the stabilizing effect of its fixed topological structure (frozen inhomogeneities in the terminology of Ref. [7]). Free energy effects dominate for $p\to 1$ in which case the network topology is nearly homogeneous and the locations and the detailed shapes of the microphase separation patterns are determined by homogeneous nucleation events which take place at random locations in the network. Network topology dominates as $p\to 0.5$ (from above) in which case the inhomogeneous density profile of the network (determined by its topology) serves as a nucleus for heterogeneous nucleation. In this case, as temperature is decreased, the crude features of the density profile remain unaffected and one observes progressive coarsening of the high-temperature pattern. The crossover between the free energy and the network topology dominated regimes appears to take place smoothly as p varies from 1 to 0.5. These behaviors are clearly observed in Fig. 2 where we present snapshots of systems created at $p=0.9$ [Figs. 2(a)–2(c)] and $p=0.6$ [Figs. 2(d)–2(f)]; while there is practically no correlation between patterns observed at different temperatures in the $p=0.9$ case, the $p=0.6$ patterns are strongly correlated. In order to quantify this observation, in the insets to these figures we introduce a quantitative measure of similarity between the (time averaged) particle density patterns $\rho_{T,T'}(\vec{x})$ taken at two different temperatures T and T' by defining the density correlation coefficient [15] $C(T,T')=(\langle\rho_T\rho_{T'}\rangle-\langle\rho_T\rangle\langle\rho_{T'}\rangle)/[\Delta(\rho_T)\Delta(\rho_{T'})]$ with $\Delta^2(\rho)=\langle\rho^2\rangle-\langle\rho\rangle^2$, where the averaging is over the area of the network. The densities were computed on a regular grid with grid size 7.5; the results did not vary qualitatively by changing the grid size as long as the grid size remained large compared to the average distance between particles and small compared to the system size. For $p=0.9$, at temperatures below $T^*_{p=0.9}=0.53\pm 0.03$, the density profile of the network undergoes massive rearrangement, a process that begins by homogeneous nucleation of the HDP. While the number of nucleation sites increases monotonously with decreasing temperature, their locations and,

therefore, the shape of the resulting density patterns are uncorrelated. Consequently, one expects fast decay of the correlation $C(T,T')$ as a function of $|T-T'|$, as is indeed observed in Figs. 2(a)–2(c). As expected, a slower decrease in $C(T,T')$ with $|T-T'|$ is observed at temperatures above $T^*_{p=0.9}$, where particles fluctuate about their initial locations whose mean position is nearly independent of temperature. An opposite trend is observed for strongly inhomogeneous networks, as shown in Figs. 2(d)–2(f) for the case $p=0.6$; while fast decrease in correlations with $|T-T'|$ is observed at $T>T^*_{p=0.6}=1.2\pm0.2$, a more moderate decrease is observed below the critical temperature. The reason for the latter behavior is that in this limit the coarse-grained density pattern is largely determined by the topology of the network and only coarsening of this pattern is observed as temperature is reduced. A corollary of the above discussion is that the correlation $C_{T'}(T,T)$ between two density patterns obtained by a cyclic change in the temperature, $T\rightarrow T'\rightarrow T$ (e.g., for $T<T^*_p$ and $T'>T^*_p$), vanishes for homogeneous networks $(p\rightarrow 1)$ but is finite for strongly inhomogeneous ones $(p\rightarrow 0.5)$. The latter behavior was observed by photon correlation spectroscopy in Ref. [15]. Both the homogeneous and the inhomogeneous regimes are clearly seen in Fig. 2(B) where we plotted $C_{T'}(T,T)$ as a function of $T<T^*_p$ for $T'=5$ and $p=0.9$ and 0.6, respectively.

We have shown that microphase separation in randomly cross-linked LJ networks is determined by the interplay of attractive forces and network topology, which resembles the interplay between thermal fluctuations and frozen inhomogeneities in polymer gels [7]. Although the present study is limited to 2D, preliminary results on three-dimensional (3D) networks indicate that many of the qualitative features reported here apply to 3D as well. Indeed, for sparsely cross-linked networks, the predicted p dependence of T^*_p is in qualitative agreement with experimental observations on NIPA/AAc gels which also exhibit microphase separation because the charged gel is stabilized against collapse in poor solvent by electrostatic repulsion and osmotic pressure of counterions [14]. However, while many polymer gels in good solvents exhibit enhancement of frozen inhomogeneities (and therefore of small-angle neutron scattering [16]) with degree of cross-linking, our LJ networks become increasingly homogeneous as the limit $p=1$ is approached. The difference can be attributed to the cross-linking process: while we start with a stretched, fully connected network and cut bonds with probability that does not depend on the state of neighboring bonds, gels which exhibit anomalously high small-angle scattering are prepared by copolymerizing monomers and cross-linkers; and since the probability of adding a monomer to the network increases with the local cross-linker concentration, the topology of the resulting gels becomes increasingly inhomogeneous with increasing cross-linker concentration. Such scattering is not observed in gels prepared by irradiation cross-linking of long polymers, indicating that the latter method results is more homogeneous networks [17].

Recently an experimental study has appeared on tetra-PEG gels formed by combining two types (TAPEG and TNPEG) of four-armed macromonomers. By varying the ratio of the two monomers from 1:1 to the highly asymmetric limit, the structure was changed from nearly homogeneous network topology to extremely inhomogeneous one [18]. While no quantitative comparison was attempted yet, these results closely resemble the variation in network structure with changing p in Fig. 2.

[1] O. Peleg *et al.*, EPL **77**, 58007 (2007).
[2] O. Peleg *et al.*, Macromolecules **41**, 3267 (2008).
[3] K. Sekimoto, N. Suematsu, and K. Kawasaki, Phys. Rev. A **39**, 4912 (1989).
[4] A. Onuki and S. Puri, Phys. Rev. E **59**, R1331 (1999).
[5] J. Bastide, L. Leibler, and J. Prost, Macromolecules **23**, 1821 (1990).
[6] A. Onuki, J. Phys. II **2**, 45 (1992).
[7] S. Panyukov and Y. Rabin, Phys. Rep. **269**, 1 (1996).
[8] J. P. Cohen Addad, *Physical Properties of Polymeric Gels*, 1st ed. (Wiley, New York, 1996).
[9] A. Moussaid *et al.*, Macromolecules **32**, 3774 (1999).
[10] S. Lay, J.-U. Sommer, and A. Blumen, J. Chem. Phys. **113**, 11355 (2000).
[11] J. A. Barker, D. Henderson, and F. F. Abraham, Physica A **106**, 226 (1981).
[12] M. Kröger *et al.*, Soft Matter **4**, 18 (2008).
[13] Supplementary information permanently available online at http://www.complexfluids.ethz.ch/gels2
[14] M. Shibayama *et al.*, J. Chem. Phys. **107**, 5227 (1997).
[15] C. Goren *et al.*, Macromolecules **33**, 5757 (2000).
[16] J. Bastide and S. J. Candau, in *The Physical Properties of Polymeric Gels*, edited by J. P. Cohen Addad (Wiley, New York, 1996), p. 143.
[17] T. Norisuye *et al.*, Polymer **43**, 5289 (2002).
[18] T. Sakai *et al.*, Macromolecules **41**, 5379 (2008).